

The intrinsic shape of galaxy bulges

J. Méndez-Abreu

Abstract The knowledge of the intrinsic three-dimensional (3D) structure of galaxy components provides crucial information about the physical processes driving their formation and evolution. In this paper I discuss the main developments and results in the quest to better understand the 3D shape of galaxy bulges. I start by establishing the basic geometrical description of the problem. Our understanding of the intrinsic shape of elliptical galaxies and galaxy discs is then presented in a historical context, in order to place the role that the 3D structure of bulges play in the broader picture of galaxy evolution. Our current view on the 3D shape of the Milky Way bulge and future prospects in the field are also depicted.

1 Introduction and overview

Galaxies are three-dimensional (3D) structures moving under the dictates of gravity in a 3D Universe. From our position on the Earth, astronomers have only the opportunity to observe their properties projected onto a two-dimensional (2D) plane, usually called the plane of the sky. Since we can neither circumnavigate galaxies nor wait until they spin around, our knowledge of the intrinsic shape of galaxies is still limited, relying on sensible, but sometimes not accurate, physical and geometrical hypotheses.

Despite the obvious difficulties inherent to measure the intrinsic 3D shape of galaxies, it is doubtless that it keeps an invaluable piece of information about their formation and evolution. In fact, astronomers have acknowledged this since galaxies were established to be *island universes* and the topic has produced an outstanding amount of literature during the last century.

J. Méndez-Abreu
School of Physics and Astronomy, University of St Andrews, North Haugh, St Andrews, KY16
9SS, UK, e-mail: jma20@st-andrews.ac.uk

In this paper I discuss the main developments and results in the quest to better understand the 3D shape of galaxy bulges. Given the limited space available in this chapter, I have not elaborated on the concept and definition of a bulge, leaving this discussion to another chapter in this volume. In the same way, I have deliberately not included the intrinsic shape of boxy/peanut (B/P) structures located in the centre of disc galaxies which some authors associate to galaxy bulges [92]. Currently it is well established that these structures are actually part of the bar and intimately related to their secular evolution [37, 34]. As bars evolve, stars can be moved perpendicular to the disc plane due to a coherent bending of the bar producing its characteristic shape [45, 94]. B/P structures share the same photometric and kinematic properties of bars [99, 50].

On the other hand, I have included a historical review of the evolution of our knowledge of the intrinsic shape of elliptical galaxies. The properties of elliptical galaxies and those of intermediate/massive galaxy bulges have been often considered to be similar [147]. This is particularly true when referring to their surface-brightness distributions and shapes. Indeed, it has been common in the literature to rely on both simulations and observations of elliptical galaxies to interpret the observational properties of bulges (e.g., [82]).

This paper is structured as follows. In Section 2 I describe the basic geometric considerations of the problem and set up the notation used throughout the chapter. In Section 3 I review our current knowledge on the intrinsic shape of both elliptical and disc galaxies. Section 4 introduces the advantages and drawbacks of studying galaxy bulges with respect to ellipticals and a historical perspective of their 3D shape measurements. In Section 5 I summarize the evolution of the concept of the Milky Way bulge and its intrinsic 3D shape. Section 6 addresses the importance of numerical simulations to understand the physical processes that shape galaxy ellipsoids. Finally, in Section 7 I sketch out the current view on the intrinsic shape of bulges and explore future prospects.

2 Setting up the Scene

This section briefly summarizes the basic notation and geometrical considerations to be used during this chapter.

Let (x, y, z) be the Cartesian coordinates on the reference system of the galaxy with the origin in the galaxy centre, the x -axis and y -axis corresponding to the principal equatorial axes of the ellipsoidal component, and the z -axis corresponding to the polar axis. Therefore, if A , B , and C are the intrinsic lengths of the ellipsoid semi-axes, the corresponding equation of the bulge on its own reference system is given by

$$\frac{x^2}{A^2} + \frac{y^2}{B^2} + \frac{z^2}{C^2} = 1 \quad (1)$$

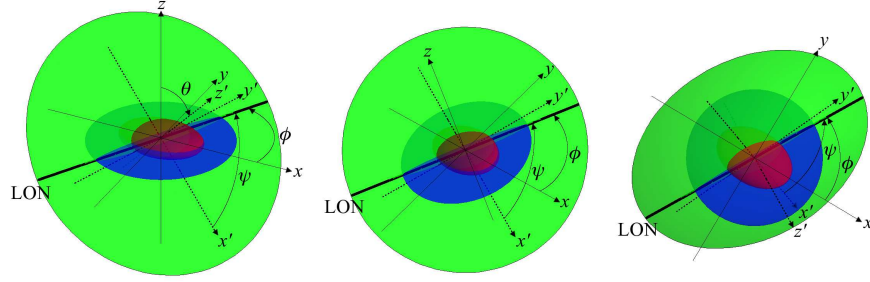


Fig. 1 Schematic three-dimensional view of the ellipsoid geometry. The bulge ellipsoid, the disc plane, and the sky plane are shown in red, blue, and green, respectively. The reference systems of both the ellipsoid and the observer as well as the LON are plotted with thin solid lines, thin dashed lines, and a thick solid line, respectively. The bulge ellipsoid is shown as seen from an arbitrary viewing angle (left panel), along the LOS (central panel), and along the polar axis (i.e., the z -axis; right panel). Extracted from [100].

Let (x', y', z') now be the Cartesian coordinates on the observer reference system. It has its origin in the galaxy centre, the polar z' -axis is along the line of sight (LOS) and points toward the galaxy. (x', y') represents the plane of the sky.

The equatorial plane (x, y) of the ellipsoid and the plane of the sky (x', y') intersect in the so-called line of nodes (LON). The angle between both planes, i.e., the angle subtended between z and z' is defined as the inclination θ of the ellipsoid. The remaining two Euler angles which allow for the transformation from the reference system of the galaxy to that of the sky are defined as: i) ϕ is the angle subtended between the x -axis and the LON in the ellipsoid equatorial plane, and ii) ψ is the angle subtended between the x' -axis and the LON in the plane of the sky. It is often useful to choose the x' -axis to be along the LON, consequently it holds that $\psi = 0$ (see Figure 1).

It is well known that the projection of a triaxial ellipsoid onto the plane of the sky describes an ellipse [38, 130, 21, 62], which is usually written as

$$\frac{x_e^2}{a^2} + \frac{y_e^2}{b^2} = 1 \quad (2)$$

where x_e and y_e represent the axes of symmetry of the projected ellipse, a and b are the corresponding semi-major and semi-minor axes of the ellipse. The observed ellipticity of the ellipse can be easily derived from the apparent axis ratio as $\varepsilon = 1 - b/a$. The x_e axis forms an angle δ with the LON (twist angle), which for convenience is usually made to correspond with the x' -axis. It is worth noting that both the apparent axis ratio ($q = b/a$) and the orientation of the ellipses (δ) depend only, and unambiguously, on the direction of the LOS, i.e., on θ , ϕ , and ψ , and on the intrinsic shape of the ellipsoid, i.e., A, B , and C , see [126] for the full derivation.

Based on this simple geometric representation, if we assume a galaxy is composed of a set of triaxial emitting ellipsoidal shells, which are concentric and coaxial (same axes of symmetry) but non-homologous (intrinsic semi-axes vary with the distance to the centre), their projections onto the plane of the sky are concentric ellipses, but non-homologous and non-coaxial. Therefore, the twisting of the galaxy isophotes can be explained just as an effect of the projection of non-homologous triaxial ellipsoids [146].

3 Historical background on the intrinsic shape of galaxies

Elliptical galaxies are structurally the simplest stellar systems where mathematical techniques can be applied to recover their intrinsic 3D shape. Thus, the huge amount of literature on the subject is not surprising. In fact, the continuously increasing availability of better measurements of the apparent axis ratios of elliptical galaxies have motivated great debate over the years. On the other hand, the similarities between the photometric properties of intermediate/massive bulges and ellipticals (e.g., [64]) have usually motivated an extrapolation of the results on the intrinsic 3D shape of ellipticals and their implications on galaxy formation and evolution onto the bulges of disc galaxies. In this section I revisit our current knowledge on the intrinsic shape of elliptical galaxies (Sect. 3.1) and, for the sake of completeness, of disc galaxies (Sect. 3.2) to put in context the historical background on the intrinsic shape of bulges.

3.1 *Intrinsic shape of elliptical galaxies*

3.1.1 Photometric approach

The first attempt to derive the intrinsic shape of elliptical galaxies was done by [73]. At that time, it was already realized the importance of relying on statistical methods to recover the 3D shape of galaxies. In fact, Hubble obtained the frequency of intrinsic short-to-long axis ratio under the assumption that elliptical galaxies were oblate ellipsoids with random orientations with respect to the LOS.

Since then, this statistical approach based on the measurement of the apparent axis ratio distribution (AARD) and the assumption that the 3D intrinsic shape is an ellipsoid of revolution, either oblate or prolate, has been extensively used in the literature. For the sake of clarity I briefly outline here the basic statistical concepts.

Let us assume the basic geometry proposed in Sect. 2 and define both the intrinsic ellipticity, $Q = B/A$, and intrinsic flattening, $F = C/A$, of the ellipsoid as the corresponding intrinsic axis ratios in the (x, y) and (x, z) planes, respectively. Therefore, in the case of either a pure oblate ($Q = 1$) or pure prolate ($Q = F$) ellipsoid the Eq. 1 can be described by one single parameter. If the polar axis of the ellipsoid forms

an angle (θ) with respect to the LOS then the apparent axis ratio of the projected ellipse can be written as

$$F^2 \sin^2 \theta + \cos^2 \theta = \begin{cases} q^2 & \text{if oblate} \\ q^{-2} & \text{if prolate} \end{cases} \quad (3)$$

Under the realistic assumption of randomly distributed orientations and using Eq. 3 where $q = q(\theta)$, the probability $P(q|F)dq$ that a galaxy with intrinsic axis ratio F is observed with an apparent axis ratio in the range $(q, q + dq)$ is

$$P(q|F)dq = \frac{\sin \theta dq}{|dq/d\theta|} \quad (4)$$

At this point, the AARD $\zeta(q)$, can be related to the intrinsic probability distribution $\xi(F)$ by

$$\zeta(q) = \int_0^1 P(q|F) \xi(F) dF \quad (5)$$

The relation between the known (observed) frequency of galaxies of apparent axis ratio $\zeta(q)$ to the unknown frequency $\xi(F)$ of galaxies with intrinsic axis ratio F can be written such as

$$\zeta(q) = \begin{cases} q \int_0^q \frac{\xi(F) dF}{\sqrt{(1-F^2)(q^2-F^2)}} & \text{if oblate} \\ q^{-2} \int_0^q \frac{\xi(F) F^2 dF}{\sqrt{(1-F^2)(q^2-F^2)}} & \text{if prolate} \end{cases} \quad (6)$$

Based on this approach and using the hypothesis of oblateness, [120] derived the intrinsic distribution of flattening $\xi(F)$ for different Hubble types ranging from ellipticals to Sc. They found that the observed axis ratios of 168 elliptical galaxies present in the Reference Catalog of Bright Galaxies (RC1) [47] were well reproduced using a skewed binomial distribution of oblate ellipsoids given by

$$\xi(F) \propto \left(1 + \frac{F - F_0}{\beta}\right)^\alpha \exp[-\alpha(F - F_0)] \quad (7)$$

with main parameters $F_0 = 0.58$ and $\beta = 0.31$ (Figure 2, left panels).

[20] used the same sample but introducing the prolate approach. Adopting the same functional form for $\xi(F)$ he found values of $F_0 = 0.40$ and $\beta = 0.71$. However, even if using arbitrary analytical representations of $\xi(F)$ can turn out in a good fit of the AARD, in principle they do not have a physical motivation. This approximation was improved by [105] by solving Eq. 6 using the non-parametric inversion technique proposed by [91]. His results show how under the hypothesis of oblateness the $\xi(F)$ distribution of [120] was correct, but he also noticed that a prolate distribution peaking at around $F \sim 0.7$ would produce a good representation of the data as well.

At the same time, some kinematic findings led to the suggestion that the structure of elliptical galaxies can be represented by neither oblate nor prolate ellipsoids of revolution. In fact, the low ratio between rotational velocity and velocity dispersion found in flat systems [14, 74, 109] or the rotation measured along the minor axis of some elliptical galaxies [123] were interpreted as resulting from a triaxial structure. From the photometric point of view, the twisting of the inner isophotes of elliptical galaxies was known since the early work of [52] and it was latter confirmed in several works [86, 30, 15].

As a consequence, [12] and [22] showed that the AARD could be satisfactorily accounted for also in terms of a distribution of triaxial ellipsoids. Nevertheless, these works still presented significant differences in the predicted number of spherical galaxies mainly due to the differences in the original samples. Other groups reached similar conclusions analysing higher quality data coming from new CCD detectors [58].

A new step forward in the methodology to recover the intrinsic 3D shape of galaxies was done by [54]. They showed how the inversion of the integral equations for oblate and prolate ellipsoids (Eq. 6) can be performed analytically, resulting in

$$\xi(F) = \frac{2}{\pi} \sqrt{1-F^2} \begin{cases} \frac{1}{F} \int_0^F \frac{qdq}{\sqrt{F^2-q^2}} \frac{d\xi}{dq} & \text{if oblate} \\ \frac{1}{F^3} \int_0^F \frac{qdq}{\sqrt{F^2-q^2}} \frac{d(q^3\xi)}{dq} & \text{if prolate} \end{cases} \quad (8)$$

Using this analytical inversion and the largest sample of galaxies to that date (2135 elliptical galaxies), [83] demonstrated how neither oblate nor prolate models could adequately reproduce the data. Contrarily, triaxial ellipsoids with intrinsic axis ratios selected from 1D Gaussians provided an adequate fit to the data. They found a best fit with $Q = 0.95$ and $F = 0.55$. A similar approach was used by [115] on a smaller sample of 171 elliptical galaxies. She used a 2D Gaussian combining both intrinsic axis ratios obtaining $Q = 0.98$ and $F = 0.69$. The same sample was later analysed by [137] using a non-parametric technique to test the triaxial hypothesis. They confirmed previous results that discarded a distribution of intrinsic shapes compatible with axisymmetric ellipsoids thus favouring triaxial distributions. Similar conclusions were reached by [116] on a larger sample using the same non-parametric approach.

During these years it became increasingly clear that the distribution of intrinsic flattenings of elliptical galaxies was broad and possibly bimodal [58, 115, 137, 116]. In fact, combining the galaxy sample described in [115] with a new sample of brightest cluster galaxies (BCGs) from [84], [138] found that the AARD of galaxies brighter than $M_B \simeq -20$ was different from that of the less luminous ones. This reflected a difference in the shape of low-luminosity and high-luminosity ellipticals: fainter ellipticals are moderately flattened and oblate, while brighter ellipticals are rounder and triaxial. Recently, [57] also found that even if both normal ellipticals and BCGs are triaxial, the latter tend to have a more prolate shape, and the tendency to prolateness is mainly driven by the central dominant (cD) galaxies present in their sample.

The next qualitative leap in studies of the intrinsic shape of elliptical galaxies happened with the advent of the Sloan Digital Sky Survey (SDSS). With respect to previous statistical analyses, SDSS improved not only the number of galaxies under study (an order of magnitude larger) but also the quality and homogeneity of the photometry. All these improvements allowed to study the dependence of the intrinsic shape with other galaxy properties such as the luminosity, colour, physical size, and environment. Using data from the SDSS-DR3 [1] [141] found that bright galaxies ($M_r \leq -21.84$) with a de Vaucouleurs profile have an AARD consistent with a triaxiality parameter in the range $0.4 < T < 0.8$, where $T = (1 - Q^2)/(1 - F^2)$, and mean flattening $0.66 < F < 0.69$. The faintest de Vaucouleurs galaxies are best fit with prolate ellipsoids ($T = 1$) with mean flattening $F = 0.51$. Using the SDSS-DR5 [2], [79] were able to reproduce the AARD by using a combination of oblate, prolate, and triaxial galaxy populations. Following the early work of [138], they assumed each population having a Gaussian distribution of their intrinsic axis ratios. The best fit to the AARD was found using a fraction of O:P:T=0.29:0.26:0.45 (Oblate:Prolate:Triaxial) with a best triaxial distribution with axis ratios $Q = 0.92$ and $F = 0.78$. In 2008, [107] used the SDSS-DR6 [3] to derive the intrinsic shape of ellipticals with the main improvement of taking into account the effects of dust extinction. They found that the AARD of elliptical galaxies shows no dependence on colour, suggesting that dust extinction is not important for this sample. The full population of elliptical galaxies was well characterized by a Gaussian distribution in the equatorial ellipticity with mean $Q = 0.89$ and a lognormal distribution of the flattening with mean $F = 0.43$, which corresponds to slightly oblate ellipsoids in agreement with [141]. In a recent paper, [114] have used the SDSS-DR8 [4] and the morphological information from Galaxy Zoo [88] finding that elliptical galaxies have a mean value of $F = 0.58$ (Figure 2, right panels). They concluded that the increase in F is mainly due to the removal of the spiral galaxy contamination thanks to the Galaxy Zoo morphologies. A historical summary in tabular form of all these measurements is shown in Table 1.

Owing to the ill-posed problem of deriving the 3D intrinsic shape of elliptical galaxies, its historical perspective is mainly weighted toward statistical methods. As previously showed in this section, the inventiveness of astronomers, the development of statistical methods, and the advent of large surveys have significantly improved our knowledge of the intrinsic shape of elliptical galaxies. Other methods based on the photometric study of individual galaxies have also been developed but to a smaller extent. One of the pioneering works to derive the intrinsic shape of an individual elliptical using its observed ellipticity and isophotal twist was done by [145]. They modelled the elliptical galaxy NGC 0523 assuming a given intrinsic density distribution and finding that the preferred models were prolate in the external regions but increasingly mixed (oblate and prolate) towards the centre. This idea was further developed by other authors using more complex models of the density distribution [55, 136]. In 2008, [31] estimated the shapes of 10 elliptical galaxies with apparent ellipticities $\varepsilon \leq 0.3$, finding that radial differences in the triaxiality parameter can be tightly constrained to values $0.29 < \Delta T < 0.54$. [32] extended

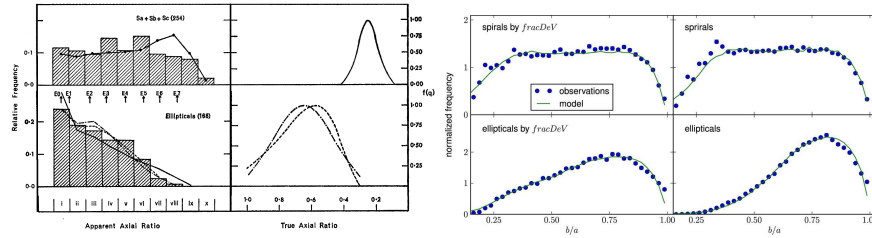


Fig. 2 Composite figure showing the evolution of the galaxy samples used in the derivation of the intrinsic shape of ellipticals and discs. Left panels: histograms of the AARD for ellipticals and spiral galaxies. The overplotted curves are predicted ratios for various assumptions of the distribution of intrinsic flattening. On the right, the assumed intrinsic distribution corresponding to the curves on the left. Extracted from [120]. Right panels: best fit models to AARD compared to the observations. Top: spirals. Bottom: ellipticals. Left: galaxies selected only by fracDeV, see [1] for definition. Right: galaxies selected by Galaxy Zoo morphology and fracDeV. Extracted from [114].

this analysis to 3 very flat galaxies with ellipticity $\varepsilon \sim 0.3$ or more. They found values of the intrinsic flattening of these galaxies around $F \sim 0.5$.

3.1.2 Kinematic approach

Determining the distribution of the 3D intrinsic shape of elliptical galaxies is also possible by combining photometric and kinematic information. In a first attempt, [21] used simple kinematical models to understand the ratio of rotational motion along both the major and minor isophotal axes of the galaxy. Using a sample of 10 ellipticals he found that elliptical galaxies were not well represented by axisymmetric oblate or prolate models. [62] revisited this approach by using a larger sample of 38 elliptical galaxies and studying the probability distribution of photometric ellipticities and kinematics misalignments. In particular, they explored the possibility that the angular momentum could not be aligned with the polar axis of the galaxy but it may have any orientation within the plane containing the short and the long axis (x, z). They found that a variety of models was able to reproduce the observations. Models with all galaxies being triaxial with well-aligned angular momentum were indistinguishable from models with all galaxies being oblate with nonaligned angular momentum.

A different standpoint to statistical studies implies an investigation into the intrinsic shape of elliptical galaxies using detailed individual dynamical modelling of the galaxy kinematics. [135] modelled the photometric and stellar kinematic measurements of three elliptical galaxies adopting a specific form for the intrinsic density and streaming motions. They found tightly constrained geometries with $0.7 < Q < 0.8$ and $0.4 < F < 0.6$. This methodology was further improved in a

Table 1 Historical summary of the intrinsic shapes of elliptical galaxies.

Year (1)	N. Galaxies (2)	Hypothesis (3)	Q (4)	F (5)	Reference (6)
1970	168	Oblate	1	0.58	[120]
1978	168	Prolate	0.4	0.4	[20]
1979	168	Oblate/Prolate	1/0.7	0.55/0.7	[105]
1980	348	Triaxial	0.81	0.62	[12]
1981	196	Oblate/Prolate/Triaxial	1/0.62/0.79	0.62/0.62/0.57	[22]
1992	2135	Triaxial	0.95	0.55	[83]
1992	171	Triaxial	0.98	0.69	[115]
2005	26994	Triaxial	0.66-0.85	0.66-0.69	[141]
2007	3922	Oblate/Prolate/Triaxial	1/0.72/0.92	0.44/0.72/0.78	[79]
2008	303390	Triaxial	0.89	0.38	[107]
2013	112100	Triaxial	0.88	0.58	[114]

Notes. (1) Year of publication of the paper. (2) Number of elliptical galaxies in each sample. (3) Hypothesis used to derive the intrinsic shape of the ellipticals. (4) Mean value of the intrinsic ellipticity. (5) Mean value of the intrinsic flattening. (6) Reference of the corresponding paper.

series of papers by Statler [131, 132, 133]. He showed how using not only their apparent shapes and velocity field misalignments, but also the velocity field asymmetry, it is possible to place tighter constraints on the intrinsic shape of ellipticals. Using this approach [9] derived the intrinsic shape of 13 elliptical galaxies finding that although photometric studies give similar results for the flattening, none is able to put real constraints on triaxiality even when large samples are studied, hence demonstrating the need to include kinematic data in the models. Figure 3 show the probability distribution of intrinsic axis ratio for 9 galaxies with significant rotation in their sample. It is clear that most of the galaxies can be well described by nearly oblate models but some of them present significant triaxiality or even prolateness. [139] investigated how well the intrinsic shape of elliptical galaxies can be recovered by fitting realistic triaxial dynamical models to simulated photometric and kinematic observations. They found that for axisymmetric galaxies, the models are able to exclude triaxiality but the intrinsic flattening is nearly unconstrained. On the other hand, the shape of triaxial galaxies can be accurately determined when additional photometric and kinematic complexity, such as the presence of isophotal twist or a kinematically decoupled core is observed.

Recently, [142] studied the intrinsic shape of the early-type galaxies described in the ATLAS3D survey [29]. Using a purely photometric approach and assuming axisymmetry, they found that the fast rotator population was much flatter than the slow rotator population, as expected from their dynamical status. Moreover, when the kinematic misalignment is included as a constraint in the analysis, they demonstrated that fast rotators are still better represented to oblate ellipsoids.

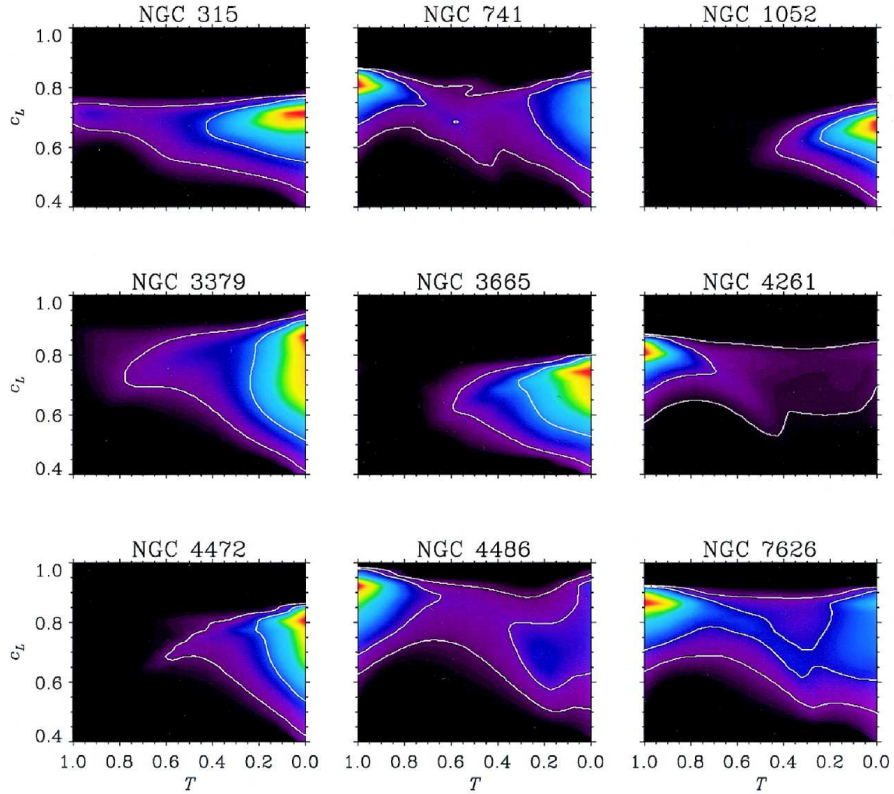


Fig. 3 Posterior probability densities in the plane of intrinsic triaxiality, T , and flattening, c_L (F in this chapter), for each of the nine galaxies that show significant rotation in [9]. Contours indicate the 68% and 95% highest posterior density regions. In each panel, round prolate galaxies are at the top left, flattened oblate galaxies at bottom right, and objects in between are triaxial. Most galaxies are well represented by oblate models but prolate and triaxial are also allowed in many galaxies, e.g., NGC 741, NGC 4486, or NGC 7626. Extracted from [9].

3.2 Intrinsic shape of disc galaxies

In this section I briefly summarise our current understanding about the intrinsic 3D shape of discs. Bulges are embedded into the disc light and axisymmetry is usually a requirement to derive the bulge intrinsic shape. However, although the discs of lenticular and spiral galaxies are often considered to be infinitesimally thin and perfectly circular, their intrinsic shape is better approximated by flattened triaxial ellipsoids.

The disc flattening, defined analogously as for ellipticals (Sect. 3.1), can be directly determined from edge-on galaxies. It depends both on the wavelength at which discs are observed and on galaxy morphological type. Indeed, galactic discs

become thicker at longer wavelengths [43, 102] and late-type spirals have thicker discs than early-type spirals [27, 69].

Determining the distribution of both the intrinsic flattening and ellipticity of discs is possible by a statistical analysis of the AARD of randomly oriented spiral galaxies. Similarly for elliptical galaxies, [120] analysed the spiral galaxies listed in the RC1. They concluded that discs are circular with a mean flattening of $\langle F \rangle = 0.25$. However, the lack of nearly circular spiral galaxies ($q \simeq 1$) rules out that discs have a perfectly axisymmetric shape. Indeed, [19], [12], and [22] have shown that discs are slightly elliptical with a mean intrinsic ellipticity $\langle 1 - Q \rangle = 0.1$. These early findings were based on the analysis of photographic plates of a few hundreds of galaxies. They were later confirmed by measuring ellipticities of several thousands of objects in CCD images and digital scans of plates obtained in wide-field surveys. [83] found that pure oblate models failed to reproduce the AARD of spiral galaxies, whereas nearly oblate models with $F \sim 0.2$ and $Q \sim 0.9$ produce a good fit with values similar to those of [120]. These values were confirmed later on by different authors [56, 5, 117]. Like the flattening, the intrinsic ellipticity depends on the morphological type and wavelength. The discs of early-type spirals are more elliptical than those of late-type spirals and their median ellipticity increases with observed wavelength [118]. Furthermore, luminous spiral galaxies tend to have thicker and rounder discs than low-luminosity spiral galaxies [107]. In [119] they studied the role of stellar mass in shaping the thickness of galaxy discs. They found that the intrinsic thickness distribution of discs has a characteristic *U-shape* and identify a limiting mass $M_* \approx 2 \times 10^9 M_\odot$ below which low-mass galaxies start to be systematically thicker. Recently, [114] analyse a sample of 92923 spiral galaxies extracted from the SDSS-DR8, and taking into account the effects of dust in their analysis, they found a distribution of flattening with mean $F = 0.27$ and ellipticity $Q = 0.22$, i.e., disc are less round than in previous studies (Figure 2, right panels).

Despite the large effort made to understand the intrinsic 3D shape of galaxy discs, it is still unclear whether the inferred slight triaxiality could be due to the presence of substructure in galaxy discs or if it really reflects truly triaxial potential in spirals.

4 The intrinsic shape of extragalactic bulges.

The study of the intrinsic shape of bulges presents similarities, advantages, and drawbacks with respect to that of elliptical galaxies. Bulges are ellipsoidal systems located in the centre of disc galaxies, thus, the main drawback with respect to elliptical galaxies is that their analysis requires the isolation of their light distributions from other structural galaxy components. However, it is worth noting that a similar problem is faced in elliptical galaxies when defining a characteristic radius to measure the global axis ratio of the galaxy [58]. The most common approach to identifying a global axis ratio for the bulge is by performing a photometric decomposition of the galaxy surface-brightness distribution. In this method, the galaxy light is usually modelled as the sum of the contributions from the different struc-

tural components, i.e., bulge and disc, and eventually lenses, bars, spiral arms, and rings [112, 85]. A number of two-dimensional parametric decomposition techniques have been developed to this aim, such as: GIM2D [125], GALFIT [108], BUDDA [46], GASP2D [98], GALPHAT [148], or IMFIT [51]. On the other hand, the main drawback on the study of galaxy bulges, i.e., the presence of other components such as the main disc, represents in turn the main advantage. The presence of the galactic disc allows for accurately constraining the inclination of the galaxy. Hence, under the assumption that the two components share the same polar axis (i.e., the equatorial plane of the disc coincides with that of the bulge) it allows for the determination of the inclination of the bulge. This is crucial to solve one of the main concerns when dealing with elliptical galaxies.

4.1 Photometric approach

Galaxy bulges were initially thought as axisymmetric ellipsoids placed at the centre of disc galaxies. The first piece of photometric evidence against this idea was given by [87]. He showed a misalignment between the major axes of the disc and bulge in M31, realising that this would be impossible if both the disc and bulge were oblate. This photometric misalignment is similar to the isophote twist observed in elliptical galaxies and used as an indication of triaxiality in these systems [146]. The extensive study undergone by [76] showed that the twisting isophotes between the central and outer parts of disc galaxies are quite common, but it was not until 1986 when [149] properly studied the deviations from axisymmetry in the bulges of spiral galaxies. They found bulge-to-disc misalignments in their sample of 11 spiral galaxies hence confirming the high incidence of non-axisymmetric bulges in ordinary spirals and placing some parallelisms with elliptical galaxies. [11] also found compelling photometric evidence for triaxiality in the bulge of NGC 4736.

The first quantitative estimation of the intrinsic 3D shape of galaxy bulges using a statistical approach was performed by [17]. They measured the bulge AARD and the misalignments between the major axes of the bulge and disc in a sample 32 S0–Sb galaxies. Under the hypothesis that discs are circular, they found that these bulges are triaxial with mean axial ratios $\langle Q \rangle = 0.86$ and $\langle F \rangle = 0.65$. Interestingly, they also demonstrated that a random projection of the probability distribution function of the bulges axis ratios fit sufficiently well to the AARD of the elliptical galaxies presented in [22]. The results were interpreted as both populations of objects having the same origin.

[59] derived the intrinsic ellipticity of bulges by analysing the deprojected apparent axis ratio of the galaxy isophotes within the bulge radius. This work did not assume any geometrical model for the galaxy but only that the disc be circular. They found $\langle Q \rangle = 0.79$ and $\langle Q \rangle = 0.71$ for the bulges of 35 early-type and 35 late-type disc galaxies, respectively. Despite the different methodologies, these results were in good agreement with previous results by [17]. Along the same lines, none of the 21 disc galaxies with morphological types between S0 and Sab studied by [106]

harbours a truly spherical bulge. They reach this conclusion by assuming bulges to be oblate ellipsoids and comparing the isophotal axis ratio in the bulge-dominated region to that measured in the disc-dominated region. A mean flattening $\langle F \rangle = 0.55$ was obtained which is slightly lower than the value found by [17].

The number of galaxy bulges under study increased by an order of magnitude with the work of [98]. They measured the structural parameters of bulges and discs of a sample of 148 early-to-intermediate spiral galaxies using a 2D photometric decomposition. They computed the probability distribution function of the intrinsic ellipticity from the bulges AARD, disc ellipticities, and misalignments between bulges and discs position angles. They suggested that about 80% of the sample bulges are triaxial ellipsoids with a mean axial ratio $\langle B/A \rangle = 0.85$, confirming that bulges are slightly triaxial structures.

The vertical extension of galaxy bulges remains usually hidden from observations except for edge-on galaxies. [103] obtained a median value of the flattening $\langle F \rangle = 0.63$ for a sample of both early- and late-type edge-on galaxies using near infrared photometry. These results match well with the early findings by [17].

As well as for elliptical galaxies a number of works have attempted to quantify the intrinsic shape of individual bulges using only photometric data. The pioneering work of [140] used a combination of geometrical deprojection and photometric inversion to work out the actual shape of the galaxy bulge in NGC 2841. They found that a family of triaxial ellipsoids with variable axis ratios is necessary to explain the photometric properties of its bulge. In 1998, [126] derived a set of equations defining the three intrinsic axes of a triaxial ellipsoid as a function of the measured geometry of a galaxy bulge and disc (axis ratios and position angles) and the unknown Euler angle ϕ (see Sect. 2 for definition). This seminal paper promoted the work of [100]. They introduced a new method to derive the intrinsic shape of bulges based upon the analytical relations between the observed and intrinsic shapes of bulges and their surrounding discs. Using the equations derived in [126] and introducing physical constraints on the accessible viewing angles, they found the following relation between the intrinsic semi-axes of the bulge and their observed properties

$$\frac{2 \sin(2\phi_C)}{F_\theta} F^2 = \sin(2\phi_C - \phi_B) \sqrt{(1 - Q^2)^2 - \sin^2 \phi_B (1 + Q^2)^2} - \sin \phi_B \cos(2\phi_C - \phi_B) (1 + Q^2)^2 \quad (9)$$

where ϕ_B , ϕ_C and F_θ are functions of the observed quantities a , b , δ , and θ , see equations 12, 13, and 43 of [100]. Therefore, Eq. 9 directly relates the intrinsic 3D shape of the bulge with its observed properties. Unfortunately, the relation between the intrinsic and projected variables also depends on the spatial position of the bulge with respect to the disc on its own reference system (i.e., on the ϕ angle) and therefore, as well as for ellipticals, a deterministic solution of the problem cannot be given. However, the statistical analysis provided in [100] allows us to obtain the probability distribution function of both semi-axis ratios, Q and F , for every single bulge, thus imposing tight constraints on its actual shape. Applying this technique to the sample of bulges presented in [98] they found a bimodal distribution of the triax-

iality parameter (Figure 4, left panel). In particular, bulges with Sérsic index $n \leq 2$ exhibit a larger fraction of oblate axisymmetric (or nearly axisymmetric) bulges, a smaller fraction of triaxial bulges, and fewer prolate axisymmetric (or nearly axisymmetric) bulges with respect to bulges with $n > 2$. Despite no correlations being found between the intrinsic shape of bulges and other properties such as bulge luminosity or velocity dispersion, the differences with the bulge surface-brightness distribution hint towards the presence of different bulge populations as suggested by [81].

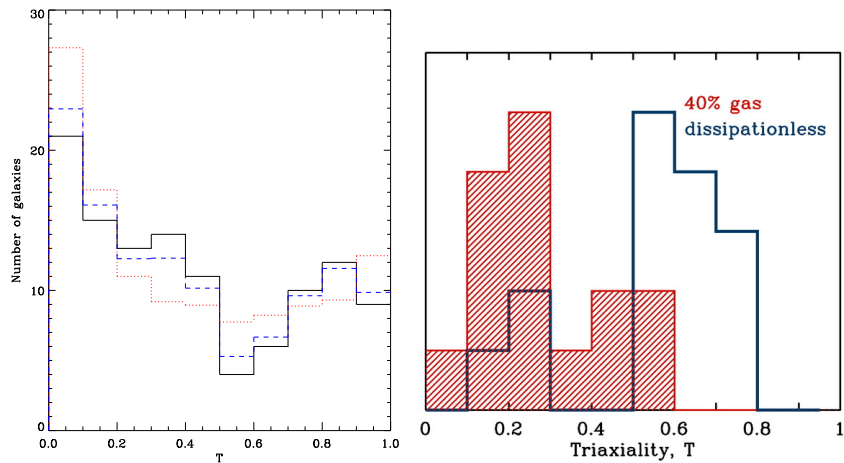


Fig. 4 Composite figure showing the similar bimodal distribution of triaxiality parameters from observations (left panel) and simulations (right panel). Left panel: distribution of the triaxiality parameter T obtained from the sample of [100] (continuous line) and for a simulated sample with both 30% and 100% of bulges hosting a nuclear bar (dashed and dotted lines), respectively. Extracted from [100]. Right panel: distribution of both dissipational (hatched histogram) and dissipationless (solid line) mergers remnant triaxiality parameter from [42]. In both panels oblate galaxies have $T = 0$, prolate galaxies have $T = 1$, and all values in between are triaxial.

4.2 Evidences of triaxiality from kinematic measurements

Early kinematic studies of galaxy bulges were shown to rotate more rapidly than elliptical galaxies [80]. In fact, the kinematic properties of many bulges are well described by dynamical models of oblate ellipsoids which are flattened by rotation with little or no anisotropy [44, 75, 60, 40, 110]. However, there are also kinematic evidences supporting a triaxial shape in a non-negligible fraction of these bulges. In 1989, two independent works of [16] and [65] reached the same conclusion about the triaxial bulge of the Sa galaxy NGC 4845. Using a combination of photomet-

ric and kinematic measurements they restrict the intrinsic axis ratio of its bulge to $Q = 0.74$ and $F = 0.6$. Their works were mainly supported by the presence of non-circular gas-motions in the galaxy centre. In a non-axisymmetric potential, the shape of the rotation curve will depend on the position of the LOS and the major axis of the non-axisymmetric component. A slowly rising rotation curve or one in which a bump of extreme velocities is seen near the centre are indications of triaxiality [65]. Based on these considerations, and building on the early work of [87], [13] demonstrated the presence of a triaxial bulge in the Andromeda galaxy (M31) by using a hydrodynamical simulation to match the observed properties of the galaxy. Further evidences for non-circular gas motion in galaxy centres can be found in [53] and [111]. Other kinematic evidence for the existence of triaxial bulges comes from the presence of velocity gradients along the galaxy minor axis. [39] found minor axis rotation in 80% of their early-type spiral sample. In a series of papers, [36, 35] found that 60% of the unbarred galaxies show a remarkable gas velocity gradient along their optical minor axis. This was achieved by combining their own data with that present in the literature (Revised Shapley-Ames Catalog of Bright Galaxies) [121].

Despite the importance of adding kinematic information to determine the intrinsic shape of the bulges, and contrary to the works on elliptical galaxies (e.g., [131]), there is not a well-established methodology to quantify the degree of triaxiality of bulges using the combined photometric and kinematic information, yet.

4.3 Polar bulges

Polar bulges, as well as their analogous polar rings [144], are elongated structures perpendicular to the plane of the galaxy disc. A common signature of both the orthogonally decoupled bulge systems and the polar ring galaxies is that both contain a structural component whose angular momentum vector is roughly parallel to the major axis of the host galaxy.

Vertical elongation is not a common feature of bulges. Indeed, most bulges can be assumed to be flattened by rotation (see Sect. 4.2). Furthermore, orthogonally decoupled bulges are usually not even *allowed* in most statistical works since the condition $A > B > C$ is commonly used, see [17]. [100] relaxed this condition and found that only 18% of the observed bulges have a probability $> 50\%$ of being elongated along the polar axis with no bulges reaching a probability $> 90\%$. In fact, to date NGC 4698 [18], NGC 4672 [122], and UGC 10043 [97] are the only spiral galaxies known to host a prominent bulge sticking out from the plane of the disc.

The case of NGC 4698 is particularly intriguing since it hosts also a polar nuclear stellar disc aligned with its polar bulge and thus perpendicular to the main disc. This galaxy was recently revisited by [41] and its intrinsic shape was derived using the methodology proposed by [100]. They found a slightly triaxial polar bulge elongated along the vertical direction with axis ratios $Q = 0.95$ and $F = 1.60$. This result agrees well with the observed kinematics presented in [18] and with a model

where the nuclear disc is the end result of the acquisition of external gas by the pre-existing triaxial bulge on the principal plane perpendicular to its shortest axis and perpendicular to the main disc of the galaxy.

5 The Intrinsic Shape of the Milky Way Bulge

Owing to its vicinity, the Galactic bulge has always been targeted as the ideal benchmark for structure, kinematic, and stellar populations studies of bulges. In fact, it can be studied at a unique level of detail, in comparison to external galaxies, thanks to the possibility of measuring the properties of individual stars. However, our *inside view* of the Galaxy generally restricts our knowledge to pencil beam areas around the Galactic centre due to either the high extinction, the crowding, or the superposition of multiple structures along the LOS, making studies of the inner Galactic regions challenging. The structure of the Galaxy has accounted for a significant amount of literature in the past and the topic has come back in the limelight in recent years. In this section I briefly review the Galactic bulge topic focusing on its intrinsic shape heading the readers to other chapters in this volume for more information about its stellar content and kinematics.

In recent decades it has become clear that the Galaxy is a barred system [25, 90] and that most likely its central regions are dominated by a boxy bulge created by vertical instabilities within the Galactic bar [49, 95, 104]. The historical evolution of our knowledge of the intrinsic structure of the Galactic bulge has been written by a succession of progressively larger scale, deeper sensitivity photometric and spectroscopic surveys.

The first attempt to understand the shape of the Galactic bulge was made by [48]. They found that models ranging from spherical to $F = 0.6$ were able to represent well both the distribution of globular clusters around the Galactic centre and the infrared isophotes observed at $2.4\mu\text{m}$ [93]. The flattening of the Galactic bulge was then further constrained with the arrival of the Infrared Astronomical Satellite (IRAS). Using IRAS data, [70] and [143] found values of the intrinsic flattening spanning $0.6 < F < 0.8$ using *JHK* near-infrared bands. Similarly, [77] found that, at first order, the Galactic bulge can be represented by an oblate ellipsoid with $F = 0.61$ using data from the Infrared Telescope (IRT).

The picture changed drastically with the advent of the COBE satellite [71]. The new striking image of the Milky Way (Figure 5) provided by the DIRBE experiment on board of COBE allowed [25], and later on [26], to find the first direct evidence for a bar at the Galactic centre. Interestingly, they also found the presence of a triaxial bulge structurally distinct from the main bar. The modelling of this triaxial bulge was performed by different teams with different sets of data in the subsequent years. Consequently, different axis ratios represented as 1:Q:F were found: 1:0.33:0.22 [49], 1:0.6:0.4 [23], 1:0.43:0.29 [129], 1:0.38:0.26 [63], 1:0.54:0.33 [89], 1:(0.3–0.4):0.3 [24], 1:0.5:0.4 [90]. In general, these values implied the Galactic bulge to

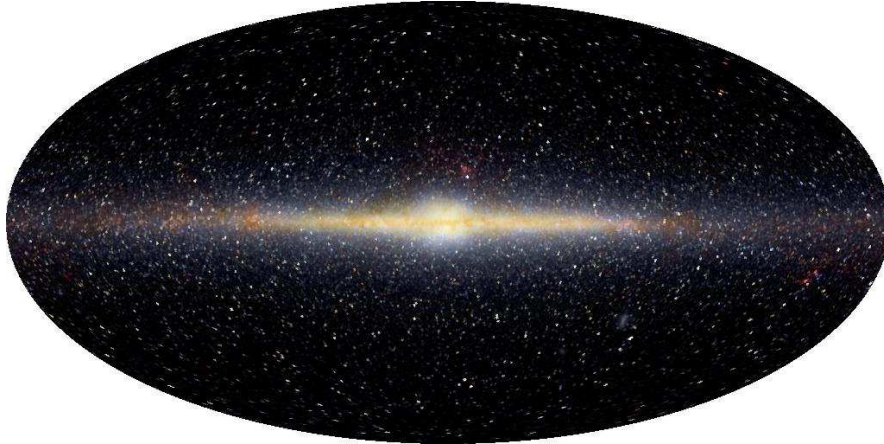


Fig. 5 False-colour image of the near-infrared sky as seen by the DIRBE. Data at 1.25, 2.2, and 3.5 μm wavelengths are represented respectively as blue, green and red colours. The image is presented in Galactic coordinates, with the plane of the Milky Way Galaxy horizontal across the middle and the Galactic centre at the centre. Credits: E. L. Wright (UCLA), The COBE Project, DIRBE, NASA.

be a triaxial structure with a tendency to prolateness, thus not in agreement with the triaxial/oblate picture outlined in Section 4 for extragalactic bulges.

Although the idea of a triaxial bulge worked well at first order, the boxy shape noticed earlier by [77] and [78] and confirmed by [49] was not recovered by a triaxial ellipsoid. In the meanwhile, different scenarios came up to explain these differences and account for the continuously increasing kinematic and stellar populations information. [6] suggested the presence of two different bars in the Galaxy by analysing data from the Two Micron All Sky Survey (2MASS) [127]. Another possible scenario was worked out by [8] suggesting a model composed by a classical bulge in the centre and a boxy bulge in the outer parts.

[124] proposed a simple model yet backed up by the high quality stellar kinematics provided by the Bulge Radial Velocity Assay (BRAVA) [113]. Using N-body simulations they found no evidence for a classical bulge in the Galaxy but the bulge appears to be only part of the bar and therefore not a separated component. Figure 6 shows that the inclusion of a classical bulge greatly worsens the model fit to the data. Models from [124] rule out that the Milky Way has a significant classical bulge with mass $>15\%$ of the disc mass.

Following this line, [95] demonstrated how the star counts measurements by [28] agrees with a scenario composed by a single bar and a boxy bulge. More recent measurements of star counts from the VISTA Variables in The Via Lactea (VVV) [67], metallicity gradients from the Abundances and Radial velocity Galactic Origins Survey (ARGOS) [104], or stellar kinematics from BRAVA have also been reconciled within this picture [66, 96].

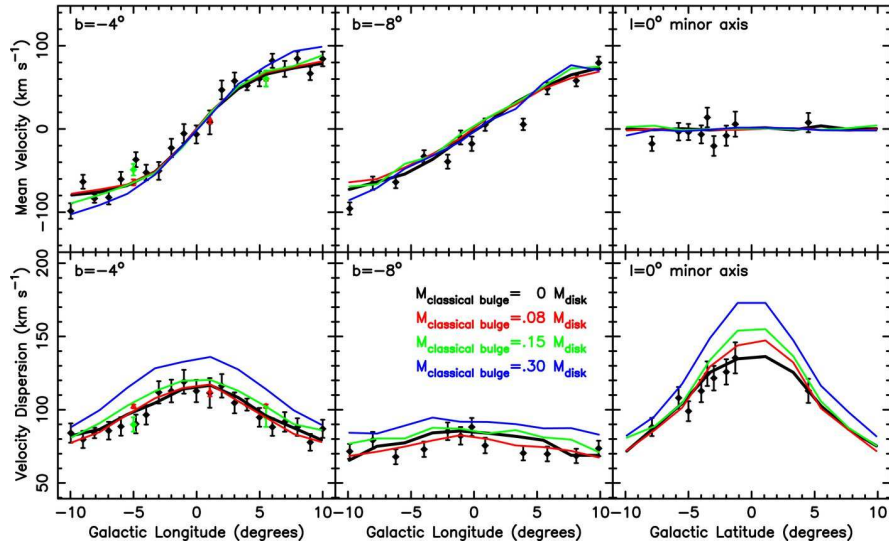


Fig. 6 Best models fits to the BRAVA stellar kinematics using different hypothesis on the classical bulge mass. Mean velocity (top panels) and velocity dispersion (lower panels) profiles of all available kinematic observations presented in [124]. The left two panels are for the Galactic latitude $b = 4^\circ$ strip; the middle two panels are for the $b = 8^\circ$; and the right two panels are for the $l = 0^\circ$ minor axis. The heavy black lines represent the model without a classical bulge. The red, green, and blue lines are for models whose classical bulges have masses of 8%, 15%, and 30%, respectively, of the disk mass. Including a classical bulge significantly worsens the model fits to the data, especially along the minor axis. Extracted from [124].

6 The 3D shape of bulges in numerical simulations.

The intrinsic shape of bulges keeps important information about their formation history, with different merger, accretion and assembly scenarios resulting in different shapes. Hence, the comparison of measured intrinsic shapes with the output from numerical simulations represents an intrinsic way to gain insights on their formation. However, numerical resolution problems have often hampered these studies and our interpretation of the shapes of bulges is usually restricted to the analysis of simulated elliptical galaxies.

[42] studied the structure of ellipsoidal remnants formed by either major (equal-mass) dissipationless or dissipational mergers of disc galaxies. They found a bimodal distribution of the triaxiality parameter in their remnant ellipticals (see right panel in Figure 4). Thus, dissipationless remnants are triaxial with a tendency to be more prolate and with a mean triaxiality parameter $T = 0.55$, whereas dissipational remnants are triaxial and tend to be much closer to oblate with triaxiality $T = 0.28$. This simulated bimodal distribution was compared by [100] to the triaxiality measured in their sample of 115 galaxy bulges (Figure 4). They concluded that both major dissipational and dissipationless mergers are required to explain the variety

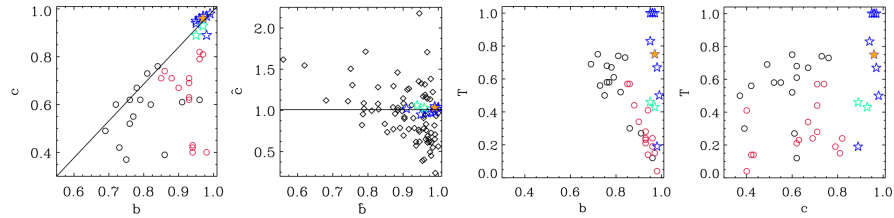


Fig. 7 Intrinsic shape of bulges and elliptical galaxies obtained from numerical simulations. A comparison with observed bulges is shown in the second panel. The blue and green stars in all panels represent the bulge remnants after suffering intermediate/minor mergers. The location of the progenitor bulges is shown with orange stars. The elliptical remnants of major mergers with pure exponential stellar discs (black circles) and containing 40% of gas (red circles) are also shown. First panel: intrinsic ellipticity b (Q in this chapter) versus the intrinsic flattening c (F in this chapter). Second panel: as panel 1 but adding the observed distribution of bulges in [100] (black diamonds). Third and fourth panels: triaxiality parameter as a function of the intrinsic ellipticity and flattening. Extracted from [134].

of shapes found for bulges. The detailed study presented by [42] is consistent with previous studies of dissipationless and dissipational mergers (e.g., [10, 72, 128]). However, the study of [68] they found how the degree of triaxiality of the elliptical remnants in dissipationless mergers also depends on the morphology of the progenitor spirals. The presence of central bulges on the progenitor galaxies produce remnants which tend to be more oblate whereas bulgeless progenitors lead to highly triaxial remnants which seems inconsistent with observations. Therefore, the comparison between simulations and observations are still subject to the range of initial conditions explored by numerical simulations.

On the other hand, even if the similarities between bulges and ellipticals have prompted observers to compare the measured properties of bulges to the properties of simulated elliptical galaxies, the formation path of bulges is likely a more complex process involving the interaction with other galaxy structural components [81, 7]. The recent work by [134] has started to fill the gap on studies about the intrinsic shape of galaxy bulges from numerical simulations. They analysed a set of N -body simulations of intermediate and minor dry mergers onto S0s to understand the structural and kinematic evolution induced by the encounters. In their experiments, the progenitor bulges are nearly spherical. The remnant bulges remain spherical as well ($Q \sim F > 0.9$), but exhibiting a wide range of triaxialities ($0.20 < T < 1.00$), remarking how the definition of this shape parameter is too sensitive to nearly spherical systems. Figure 7 (second panel) shows how the axis ratios derived from these simulations (open stars) are hardly reconcilable with the observations (black diamonds) by [100]. Still, the strong triaxiality agrees with the structure of elliptical remnants resulting from major-to-intermediate mergers [42].

7 Concluding remarks and future prospects

I present here a review of our current understanding of the intrinsic 3D shape of galaxy bulges. The approach taken in this review is largely observational and follows the historical development of the field. Thus, a journey through the past and present of our knowledge on the intrinsic shape of other galaxy ellipsoids such as elliptical galaxies or galaxy discs was needed to put the problem in context. The major conclusions of this review are:

- The observational data representing the whole population of elliptical galaxies is consistent with a mixed model, combining partly oblate and partly prolate galaxies, although a more likely alternative point towards at least some fraction of the ellipticals being triaxial ellipsoids. Triaxiality is also supported by several photometric and kinematics properties, as well as for detailed modelling of individual galaxies.
- The intrinsic shape of ellipticals shows a dependence on galaxy luminosity. Bright ellipticals are in general triaxial with a tendency to be rounder whereas faint ellipticals are more flattened with a tendency to be oblate ellipsoids.
- Even if uncertainties due to the lack of number statistics have been overcome with the advent of recent surveys, the data can still be reproduced by a wide variety of intrinsic shape distributions. Furthermore, a proper interpretation of the data is complicated by the fact that the AARD and kinematic misalignments are often a function of the radius. Therefore it is generally impossible to characterize the full shape of a single elliptical galaxy with only one or two parameters.
- Galaxy discs are, in general, well represented by nearly oblate models with $Q \sim 0.9$. Their intrinsic flattening is also well constrained to values spanning $0.2 < F < 0.3$.
- The population of galaxy bulges can be modelled as slightly triaxial ellipsoids with a tendency to be oblate. This population has typical intrinsic flattenings of $F \sim 0.65$. However, individual galaxies can have a variety of intrinsic flattenings with some extreme cases sticking out the plane of the disc, these are called polar bulges.
- The distribution of the triaxiality parameter of galaxy bulges is strongly bimodal. This bimodality is driven by bulges with Sérsic index $n > 2$. According to numerical simulations they can be explained assuming a combination of major dissipational and dissipationless mergers during their formation.
- Despite previous findings showing a triaxial bulge in the Milky Way, more recent studies have found that is more likely a boxy bulge produced by the vertical instabilities of the Galactic bar. Owing to recent kinematic measurements a classical bulge with mass $> 15\%$ of the disc mass can be ruled out.

Despite the study of the intrinsic shape of elliptical galaxies has a long track record, our knowledge of the 3D shape of bulges is still in its infancy. Therefore, further work on the topic is needed to fully exploit its possibilities. A few guidelines to this future prospects are outlined in the following:

- From a photometric point of view, even if new methodologies have been developed they need to be applied to larger samples of galaxy bulges. The number of elliptical galaxies recently analysed to recover their intrinsic shape is several orders of magnitude larger than the current samples of galaxy bulges. Large number statistics have led to the discovery of important relations for elliptical galaxies, such as the different shapes of bright and faint ellipticals, and similar studies can be crucial for galaxy bulges. This is particularly relevant in the current picture of bulge formation with a different population of classical and pseudobulges dependent of the galaxy mass [61].
- An even more promising path, already explored in elliptical galaxies, is the use of combined information from photometric and kinematic data. In particular, the common use of integral field spectroscopy is now providing an exquisite detail of the stellar and gaseous kinematics on large sample of galaxies. This wealth of information together with the development of galaxy dynamical modelling can provide a proper understanding of the intrinsic shape of galaxy bulges.
- It is doubtless that the comparison of the derived intrinsic shape of bulges with the state-of-the-art numerical simulations is a promising way to gain insights on the formation and evolution of bulges. However, there is still a lack of simulations with a large variety of initial and physical conditions interested on a structural analysis of the different galaxy components, and in particular, in the intrinsic shape evolution of galaxy bulges.
- Historically, galaxy bulges were thought as single-component objects at the centre of galaxies. This picture is now questioned since different bulge types with different formation paths have been found coexisting within the same galaxy (see [101] and reference therein). A proper separation of different bulge types, as well as the identification of possible unresolved nuclear structures such as bars, rings, etc, must be accounted for to improve our knowledge on bulge formation and evolution.
- The study of the intrinsic shape of elliptical galaxies at high redshift has recently suffered a boost thanks to the arrival of high spatial resolution surveys on large fields of view (see [33] and reference therein). This kind of studies can provide an in-situ view of galaxy evolution and their application to the intrinsic shape of bulges will be key to further progress on this topic.

Acknowledgements JMA acknowledges support from the European Research Council Starting Grant (SEDMorph; P.I. V. Wild).

References

1. Abazajian K., et al., 2005, *AJ*, 129, 1755
2. Adelman-McCarthy J. K., et al., 2007, *ApJS*, 172, 634
3. Adelman-McCarthy J. K., et al., 2008, *ApJS*, 175, 297
4. Aihara H., et al., 2011, *ApJS*, 193, 29
5. Alam, S. M. K. & Ryden, B. S. 2002, *ApJ*, 570, 610

6. Alard C., 2001, *A&A*, 379, L44
7. Athanassoula E., 2005, *MNRAS*, 358, 1477
8. Babusiaux C., et al., 2010, *A&A*, 519, A77
9. Bak J., Statler T. S., 2000, *AJ*, 120, 110
10. Barnes, J. E. 1992, *ApJ*, 393, 484
11. Beckman J. E., Varela A. M., Munoz-Tunon C., Vilchez J. M., Cepa J., 1991, *A&A*, 245, 436
12. Benacchio, L. & Galletta, G. 1980, *MNRAS*, 193, 885
13. Berman, S. 2001, *A&A*, 371, 476
14. Bertola, F. & Capaccioli, M. 1975, *ApJ*, 200, 439
15. Bertola, F. & Galletta, G. 1979, *A&A*, 77, 363
16. Bertola, F., Zeilinger, W. W., & Rubin, V. C. 1989, *ApJ*, 345, L29
17. Bertola, F., Vietri, M., & Zeilinger, W. W. 1991, *ApJ*, 374, L13
18. Bertola F., Corsini E. M., Beltrán J. C. V., Pizzella A., Sarzi M., Cappellari M., Funes S. J., J. G., 1999, *ApJ*, 519, L127
19. Binggeli, B. 1980, *A&A*, 82, 289
20. Binney, J. 1978, *MNRAS*, 183, 501
21. Binney, J. 1985, *MNRAS*, 212, 767
22. Binney, J. & de Vaucouleurs, G. 1981, *MNRAS*, 194, 679
23. Binney J., Gerhard O., Spergel D., 1997, *MNRAS*, 288, 365
24. Bissantz N., Gerhard O., 2002, *MNRAS*, 330, 591
25. Blitz L., Spergel D. N., 1991, *ApJ*, 370, 205
26. Blitz L., 1993, *Natur*, 364, 757
27. Bottinelli, L., Gouguenheim, L., Paturel, G., & de Vaucouleurs, G. 1983, *A&A*, 118, 4
28. Cabrera-Lavers A., Hammersley P. L., González-Fernández C., López-Corredoira M., Garzón F., Mahoney T. J., 2007, *A&A*, 465, 825
29. Cappellari M., et al., 2011, *MNRAS*, 413, 813
30. Carter, D. 1978, *MNRAS*, 182, 797
31. Chakraborty, D. K., Singh, A. K., & Gaffar, F. 2008, *MNRAS*, 383, 1477
32. Chakraborty D. K., Diwakar A. K., Pandey S. K., 2011, *MNRAS*, 412, 585
33. Chang Y.-Y., et al., 2013, *ApJ*, 773, 149
34. Chung A., Bureau M., 2004, *AJ*, 127, 3192
35. Coccato, L., Corsini, E. M., Pizzella, A., & Bertola, F. 2005, *A&A*, 440, 107
36. Coccato, L., Corsini, E. M., Pizzella, A., et al. 2004, *A&A*, 416, 507
37. Combes F., Sanders R. H., 1981, *A&A*, 96, 164
38. Contopoulos G., 1956, *ApJ*, 124, 643
39. Corsini, E. M., Pizzella, A., Coccato, L., & Bertola, F. 2003, *A&A*, 408, 873
40. Corsini, E. M., Pizzella, A., Sarzi, M., et al. 1999, *A&A*, 342, 671
41. Corsini E. M., Méndez-Abreu J., Pastorello N., Dalla Bontà E., Morelli L., Beifiori A., Pizzella A., Bertola F., 2012, *MNRAS*, 423, L79
42. Cox, T. J., Dutta, S. N., Di Matteo, T., et al. 2006, *ApJ*, 650, 791
43. Dalcanton, J. J. & Bernstein, R. A. 2002, *AJ*, 124, 1328
44. Davies, R. L. & Illingworth, G. 1983, *ApJ*, 266, 516
45. Debattista V. P., Carollo C. M., Mayer L., Moore B., 2004, *ApJ*, 604, L93
46. de Souza, R. E., Gadotti, D. A., & dos Anjos, S. 2004, *ApJS*, 153, 411
47. de Vaucouleurs, G. & de Vaucouleurs, A. 1964, *Reference Catalogue of Bright Galaxies*, Austin: University of Texas Press
48. de Vaucouleurs G., Pence W. D., 1978, *AJ*, 83, 1163
49. Dwek E., et al., 1995, *ApJ*, 445, 716
50. Erwin P., Debattista V. P., 2013, *MNRAS*, 431, 3060
51. Erwin P., 2014, *arXiv*, arXiv:1408.1097
52. Evans D. S., 1951, *MNRAS*, 111, 526
53. Falcón-Barroso, J., Bacon, R., Bureau, M., et al. 2006, *MNRAS*, 369, 529
54. Fall S. M., Frenk C. S., 1983, *AJ*, 88, 1626
55. Fasano, G. 1995, *Astrophysical Letters and Communications*, 31, 205
56. Fasano, G., Amico, P., Bertola, F., Vio, R., & Zeilinger, W. W. 1993, *MNRAS*, 262, 109

57. Fasano, G., Bettoni, D., Ascaso, B., et al. 2010, MNRAS, 294
58. Fasano, G. & Vio, R. 1991, MNRAS, 249, 629
59. Fathi, K. & Peletier, R. F. 2003, A&A, 407, 61
60. Fillmore, J. A. 1986, AJ, 91, 1096
61. Fisher D. B., Drory N., 2011, ApJ, 733, L47
62. Franx, M., Illingworth, G., & de Zeeuw, T. 1991, ApJ, 383, 112
63. Freudreich H. T., 1998, ApJ, 492, 495
64. Gadotti D. A., 2009, MNRAS, 393, 1531
65. Gerhard, O. E., Vietri, M., & Kent, S. M. 1989, ApJ, 345, L33
66. Gerhard O., Martinez-Valpuesta I., 2012, ApJ, 744, L8
67. Gonzalez O. A., Rejkuba M., Minniti D., Zoccali M., Valenti E., Saito R. K., 2011, A&A, 534, L14
68. González-García, A. C. & Balcells, M. 2005, MNRAS, 357, 753
69. Guthrie, B. N. G. 1992, A&As, 93, 255
70. Harmon R., Gilmore G., 1988, MNRAS, 235, 1025
71. Hauser M. G., et al., 1990, ASSL, 166, 19
72. Hernquist, L. 1992, ApJ, 400, 460
73. Hubble, E. P. 1926, ApJ, 64, 321
74. Illingworth, G. 1977, ApJ, 218, L43
75. Jarvis B. J., Freeman K. C., 1985, ApJ, 295, 324
76. Kent S. M., 1984, ApJS, 56, 105
77. Kent S. M., Dame T. M., Fazio G., 1991, ApJ, 378, 131
78. Kent S. M., 1992, ApJ, 387, 181
79. Kimm, T. & Yi, S. K. 2007, ApJ, 670, 1048
80. Kormendy, J. & Illingworth, G. 1982, ApJ, 256, 460
81. Kormendy, J. & Kennicutt, Jr., R. C. 2004, ARAA, 42, 603
82. Kormendy J., Bender R., 2012, ApJS, 198, 2
83. Lambas, D. G., Maddox, S. J., & Loveday, J. 1992, MNRAS, 258, 404
84. Lauer T. R., Postman M., 1994, ApJ, 425, 418
85. Laurikainen, E., Salo, H., & Buta, R. 2005, MNRAS, 362, 1319
86. Liller M. H., 1960, ApJ, 132, 306
87. Lindblad, B. 1956, Stockholms Observatoriums Annaler, 19, 7
88. Lintott C., et al., 2011, MNRAS, 410, 166
89. López-Corredoira M., Hammersley P. L., Garzón F., Simonneau E., Mahoney T. J., 2000, MNRAS, 313, 392
90. López-Corredoira M., Cabrera-Lavers A., Gerhard O. E., 2005, A&A, 439, 107
91. Lucy L. B., 1974, AJ, 79, 745
92. Lütticke R., Dettmar R.-J., Pohlen M., 2000, A&A, 362, 435
93. Maihara T., Oda N., Sugiyama T., Okuda H., 1978, PASJ, 30, 1
94. Martinez-Valpuesta I., Shlosman I., Heller C., 2006, ApJ, 637, 214
95. Martinez-Valpuesta I., Gerhard O., 2011, ApJ, 734, L20
96. Martinez-Valpuesta I., Gerhard O., 2013, ApJ, 766, L3
97. Matthews L. D., de Grijs R., 2004, AJ, 128, 137
98. Méndez-Abreu, J., Aguerri, J. A. L., Corsini, E. M., & Simonneau, E. 2008, A&A, 478, 353
99. Méndez-Abreu J., Corsini E. M., Debattista V. P., De Rijcke S., Aguerri J. A. L., Pizzella A., 2008, ApJ, 679, L73
100. Méndez-Abreu J., Simonneau E., Aguerri J. A. L., Corsini E. M., 2010, A&A, 521, A71
101. Méndez-Abreu, J., Debattista, V. P., Corsini, E. M., & Aguerri, J. A. L. 2014, A&A, 572, AA25
102. Mitronova, S. N., Karachentsev, I. D., Karachentseva, V. E., Jarrett, T. H., & Kudrya, Y. N. 2004, Bull. Special Astrophys. Obs., 57, 5
103. Mosenkov, A. V., Sotnikova, N. Y., & Reshetnikov, V. P. 2010, MNRAS, 401, 559
104. Ness M., et al., 2013, MNRAS, 432, 2092
105. Noerdlinger P. D., 1979, ApJ, 234, 802
106. Noordermeer, E. & van der Hulst, J. M. 2007, MNRAS, 376, 1480

107. Padilla, N. D. & Strauss, M. A. 2008, MNRAS, 388, 1321
108. Peng, C. Y., Ho, L. C., Impey, C. D., & Rix, H. 2002, AJ, 124, 266
109. Peterson C. J., 1978, ApJ, 222, 84
110. Pignatelli, E., Corsini, E. M., Vega Beltrán, J. C., et al. 2001, MNRAS, 323, 188
111. Pizzella, A., Corsini, E. M., Sarzi, M., et al. 2008, MNRAS, 387, 1099
112. Prieto, M., Aguerri, J. A. L., Varela, A. M., & Muñoz-Tuñón, C. 2001, A&A, 367, 405
113. Rich R. M., Reitzel D. B., Howard C. D., Zhao H., 2007, ApJ, 658, L29
114. Rodríguez S., Padilla N. D., 2013, MNRAS, 434, 2153
115. Ryden, B. 1992, ApJ, 396, 445
116. Ryden, B. S. 1996, ApJ, 461, 146
117. Ryden, B. S. 2004, ApJ, 601, 214
118. Ryden, B. S. 2006, ApJ, 641, 773
119. Sánchez-Janssen, R., Méndez-Abreu, J., & Aguerri, J. A. L. 2010, MNRAS, 406, L65
120. Sandage, A., Freeman, K. C., & Stokes, N. R. 1970, ApJ, 160, 831
121. Sandage A., Tammann G. A., 1981, A Revised Shapley-Ames Catalog of Bright Galaxies (Washington: Carnegie Institution) (CAG)
122. Sarzi M., Corsini E. M., Pizzella A., Vega Beltrán J. C., Cappellari M., Funes J. G., Bertola F., 2000, A&A, 360, 439
123. Schechter, P. L. & Gunn, J. E. 1979, ApJ, 229, 472
124. Shen J., Rich R. M., Kormendy J., Howard C. D., De Propris R., Kunder A., 2010, ApJ, 720, L72
125. Simard, L. 1998, in ASP Conf. Ser., Vol. 145, Astronomical Data Analysis Software and Systems VII, ed. R. Albrecht, R. N. Hook, & H. A. Bushouse. San Francisco: Astronomical Society of the Pacific, 108
126. Simonneau, E., Varela, A. M., & Munoz-Tunon, C. 1998, Nuovo Cimento B Serie, 113, 927
127. Skrutskie M. F., et al., 2006, AJ, 131, 1163
128. Springel, V. 2000, MNRAS, 312, 859
129. Stanek K. Z., Udalski A., Szymański M., Kałużyński J., Kubiak Z. M., Mateo M., Krzemiński W., 1997, ApJ, 477, 163
130. Stark A. A., 1977, ApJ, 213, 368
131. Statler, T. S. 1994, ApJ, 425, 458
132. Statler, T. S. & Fry, A. M. 1994, ApJ, 425, 481
133. Statler T. S., 1994, ApJ, 425, 500
134. Tapia T., et al., 2014, A&A, 565, A31
135. Tenjes, P., Busarello, G., Longo, G., & Zaggia, S. 1993, A&A, 275, 61
136. Thakur P., Chakraborty D. K., 2001, MNRAS, 328, 330
137. Tremblay B., Merritt D., 1995, AJ, 110, 1039
138. Tremblay, B. & Merritt, D. 1996, AJ, 111, 2243
139. van den Bosch, R. C. E. & van de Ven, G. 2009, MNRAS, 398, 1117
140. Varela, A. M., Munoz-Tunon, C., & Simonneau, E. 1996, A&A, 306, 381
141. Vincent R. A., Ryden B. S., 2005, ApJ, 623, 137
142. Weijmans A.-M., et al., 2014, MNRAS, 444, 3340
143. Whitelock P., Feast M., Catchpole R., 1991, MNRAS, 248, 276
144. Whitmore B. C., Lucas R. A., McElroy D. B., Steiman-Cameron T. Y., Sackett P. D., Olling R. P., 1990, AJ, 100, 1489
145. Williams, T. B. 1981, ApJ, 244, 458
146. Williams T. B., Schwarzschild M., 1979, ApJ, 227, 56
147. Wyse, R. F. G., Gilmore, G., & Franx, M. 1997, ARAA, 35, 637
148. Yoon, I., Weinberg, M. D., & Katz, N. 2011, MNRAS, 414, 1625
149. Zaritsky, D. & Lo, K. Y. 1986, ApJ, 303, 66